

Modern Physics Letters A
 © World Scientific Publishing Company

THERMAL PHOTONS IN STRONG INTERACTIONS

RALF RAPP

*Cyclotron Institute and Department of Physics, Texas A&M University
 College Station, Texas 77843-3366, U.S.A.
 email:rapp@comp.tamu.edu*

Received (Day Month Year)

Revised (Day Month Year)

A brief survey is given on the current status of evaluating thermal production of photons from a strongly interacting medium. Emphasis is put on recent progress in assessing equilibrium emission rates in both hadronic and quark-gluon matter. We also give an update on the status of comparing theoretical calculations with experimental data from heavy-ion collisions at the SPS, as well as prospects for RHIC. Finally, applications of photon rate calculations to color superconducting quark matter are discussed.

Keywords: thermal photon rates; QCD matter; relativistic heavy-ion collisions

PACS Nos.: include PACS Nos.

1. Introduction

Electromagnetic probes have a long and extremely successful history as valuable agents of the structure of strongly interacting objects. Many collective phenomena in atomic nuclei have been discovered through gamma ray spectroscopy, and, at much higher energies, deep inelastic scattering of electrons has lead to establishing quarks as the elementary building blocks of the nucleon, and is still being intensely used at Jefferson Laboratory to explore its nonperturbative structure. Furthermore, the emission of photons and dileptons has provided key insights into the dynamical environments created in heavy-ion collisions (see, *e.g.*, Refs. ^{1,2} for early works and Refs. ^{3,4,5,6,7} for extensive recent reviews). Here one hopes to infer properties of transient stages of highly excited matter such as its temperature or in-medium modifications of its underlying degrees of freedom. In this Brief Review we will focus on the role of thermal photons in probing hot and dense strongly interacting matter, with emphasis on recent developments rather than a complete account as has been given elsewhere⁵.

Emission rate calculations provide key input for the identification of thermal radiation from both compact stars and high-energy heavy-ion collisions, and thus for the search of new states of matter in these systems. Whereas for stars, due to their macroscopic dimension, essentially all emitted photons are of a (quasi-) ther-

mal origin, this is not the case for heavy-ion collisions. Corresponding transverse-momentum (q_t) spectra of *direct* photons, *i.e.*, those that are not due to final-state hadron decays, can be roughly decomposed into the following regimes: at sufficiently high q_t , *prompt* photons from initial nucleon-nucleon (N - N) collisions prevail, due to a characteristic power-law dependence on q_t , calculable in perturbative Quantum Chromodynamics (pQCD). Towards lower q_t , radiation from a hot and dense medium is expected to take over. The high- q_t part of the thermal spectrum will be most sensitive to the hottest phases of the produced medium, whereas at low q_t hadron gas (HG) emission is likely to dominate^a. To unfold the various components in the spectra a reliable calculation of the thermal emission rates from both the QGP and HG is mandatory, which furthermore need to be convoluted over the space-time evolution of the matter (affecting both yield and slope of the thermal components in different ways). The emission rates are also of interest in their own right, as they, in principle, encode information on the elementary excitations and their in-medium properties in the respective phase^b.

The article is organized as follows. In Sect. 2 we present the current status of evaluating thermal emission rates from both hadronic and QGP phases, highlighting recent achievements. The latter include a complete leading-order result for the QGP (Sect. 2.1), and new production channels within flavor- $SU(3)$ in the HG (Sect. 2.2). In Sect. 3 we turn to applications of model calculations to ultrarelativistic heavy-ion collisions (URHICs). We first give a brief account of nonthermal sources (Sect. 3.1), as well as of hydrodynamical simulations which are the natural space-time framework over which to convolute thermal rates. This is followed by comparisons of up-to-date calculations to (very) recent data from the Super-Proton-Synchrotron (SPS) at CERN and the Relativistic Heavy-Ion Collider (RHIC) at BNL, as well as possible interpretations thereof, and future prospects (Sec. 3.2). In Sect. 4 we discuss evaluations of thermal photon emissivities from color-superconducting quark matter at high densities and low temperatures, which could have some bearing on astrophysical contexts of supernovae or compact stars. We finish with concluding remarks in Sect. 5.

2. Thermal Photon Emission Rates

Commonly employed formalisms to calculate electromagnetic (e.m.) emission spectra from a thermal medium are finite-temperature field theory and kinetic theory. To leading order (LO) in the e.m. coupling, α_{em} , the field-theoretic expression for the emission rate per unit 4-volume, R , can be cast into the form

$$q_0 \frac{dR_\gamma}{d^3q} = -\frac{\alpha_{\text{em}}}{\pi^2} f^B(q_0; T) \text{Im}\Pi_{\text{em}}^T(q_0 = q; T) . \quad (1)$$

^aThere is also a contribution from a "pre-equilibrium" phase during which re-interactions have not yet thermalized the matter.

^bEven though dilepton invariant-mass spectra allow a more direct access to in-medium vector-spectral densities, it should be emphasized that photons and dileptons are intimately related.

It is exact in the strong interactions which are encoded in the e.m. current-current correlation function (or photon selfenergy), Π_{em} (for real photons, *i.e.*, at invariant mass $M^2 = q_0^2 - q^2 = 0$, only transverse polarizations contribute). In kinetic theory, the rate for a process of type $1+2 \rightarrow 3+\gamma$ reads

$$q_0 \frac{dR_\gamma}{d^3q} = \int \left(\prod_{i=1}^3 \frac{d^3p_i}{2(2\pi)^3 E_i} \right) (2\pi)^4 \delta^{(4)}(p_1 + p_2 - p_3 - q) |\mathcal{M}|^2 \frac{f(E_1)f(E_2)[1 \pm f(E_3)]}{2(2\pi)^3} \quad (2)$$

which is convenient if pertinent scattering amplitudes, \mathcal{M} , are evaluated in a perturbative expansion. Nonperturbative (model) calculations at low and intermediate energies, on the other hand, are more amenable to the correlator formulation, Eq.(1). In the hadronic medium, *e.g.*, Π_{em} can be directly related to vector-meson spectral functions within the vector dominance model (VDM).

2.1. Quark-Gluon Plasma

First perturbative calculations of the photon production rate from an equilibrated QGP at zero net baryon density (*i.e.*, at quark chemical potential $\mu_q = 0$) have been performed by several groups starting more than 20 years ago^{2,8}. It was soon realized⁹ that forward infrared singularities require resummed thermal propagators for the exchanged partons. For the simplest scattering diagrams depicted in the upper left panel of Fig. 1, the pertinent result, for large values of $x = q_0/T$ and two massless quark flavors (u and d), can be written as^{10,11}

$$q_0 \frac{dR_\gamma}{d^3q} = \frac{5}{9} \frac{\alpha \alpha_S}{2\pi^2} T^2 e^{-x} \ln \left(1 + \frac{2.912}{4\pi\alpha_s} x \right) \quad (3)$$

(an additive “1” has been introduced in the argument of the logarithm to enable extrapolation to small x ¹⁰). As noticed in Ref. ¹² (see also Ref. ¹³), Eq. (3) does not yet comprise the full result to leading order in the strong coupling constant α_s . Due to collinear singularities, Bremsstrahlung as well as pair annihilation graphs (cf. lower left panel of Fig. 1) contribute at the same order as the resummed $2 \rightarrow 2$ processes. The full result, which also necessitates the incorporation of Landau-Pomeranchuk-Migdal (LPM) interference effects, has been computed in Ref. ¹⁴ as

$$q_0 \frac{dR_\gamma}{d^3q} = \frac{5}{9} \frac{\alpha \alpha_S}{2\pi^2} T^2 f^F(x) \left[\ln \left(\frac{\sqrt{3}}{g} \right) + \frac{1}{2} \ln(2x) + C_{22}(x) + C_{brems}(x) + C_{ann}(x) \right], \quad (4)$$

with convenient parameterizations of the 3 functions C given by¹⁴

$$C_{22}(x) = \frac{0.041}{x} - 0.3615 + 1.01e^{-1.35x} \quad (5)$$

$$C_{brems}(x) + C_{ann}(x) = 0.633x^{-1.5} \ln(12.28 + 1/x) + \frac{0.154x}{(1 + x/16.27)^{0.5}}. \quad (6)$$

The right panel of Fig. 1 shows the individual contributions to the photon production rate corresponding to Eq. (4) (multiplied by an extra phase space factor $4\pi q^2$). In the for phenomenological applications interesting range ($x \gtrsim 4$) the

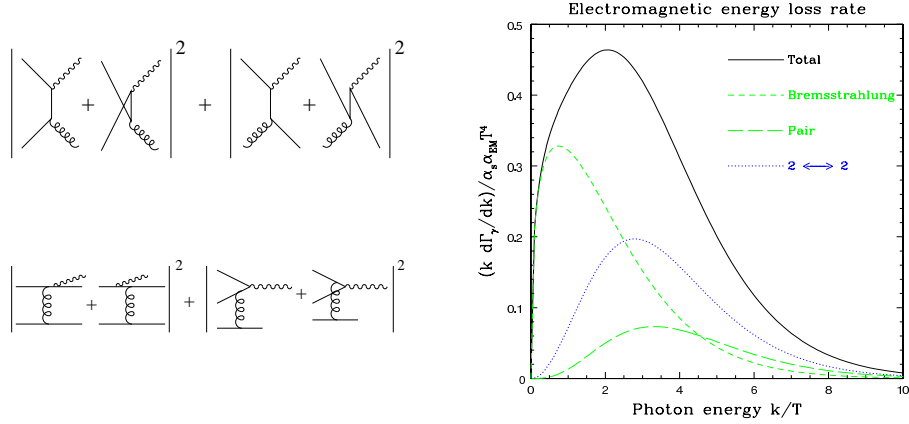
4 *Ralf Rapp*

Fig. 1. Left panel: leading-order diagrams for photon production from a QGP, taken from Ref. ¹⁴ (upper panel: $2 \rightarrow 2$ scattering; lower panel: Bremsstrahlung and pair annihilation); right panel: pertinent contributions to the photon production rate (multiplied by a phase space factor $4\pi q^2$) in a complete LO calculation with $\alpha_s=0.2$ ¹⁴.

Bremsstrahlung and pair annihilation processes augment the rate from $2 \rightarrow 2$ scattering by about a factor of 2 (see also right panel of Fig. 3 below).

Photon production from a QGP at finite net quark density ($\mu_q > 0$) has been investigated for the tree-level diagrams in the upper left panel in Fig. 1 including resummed parton propagators in Ref. ¹⁵. To a good approximation, the net effect can be represented by replacing the factor T^2 in Eq. (3) by $(T^2 + \mu_q^2/\pi^2)$. Even under conditions for heavy-ion collisions at the SPS, where QGP formation at relatively high baryon density is conceivable, with $(\mu_q, T) \simeq (100, 200)$ MeV, the μ_q^2 term amounts to a rather moderate correction (less than 5%).

In the not too far future one hopes to obtain nonperturbative information on photon production from a thermal QCD medium from first principles via QCD lattice calculations. At the moment, these calculations are available for the e.m. correlation function at finite invariant mass M ¹⁶, *i.e.*, for dilepton production. In the limit of small masses one presently finds a less singular behavior than expected from perturbative calculations employing hard-thermal-loop resummation techniques¹⁷, implying a significant suppression of photon production rates. More definite conclusions have to await the use of larger lattices to improve infrared sensitivities of the simulations.

2.2. Hadronic Matter

The study of thermal photon radiation from a hadronic gas is usually carried out within effective Lagrangians. Constraints on the interaction vertices can, to a certain extent, be imposed by symmetry principles (*e.g.*, e.m. gauge and chiral invariance), and coupling constants are estimated by adjustment to measured decay branchings in the vacuum. Thus, for the temperature ranges relevant to practical applications,

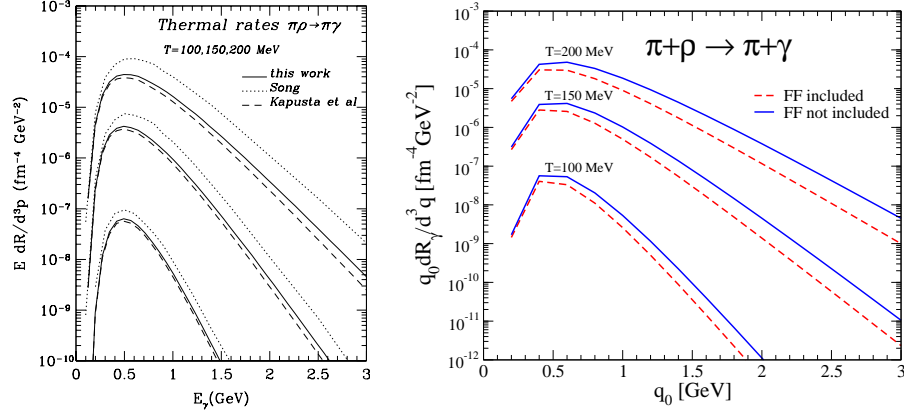


Fig. 2. Thermal photon production from inclusive $\pi\rho \rightarrow \pi\gamma$ processes at the 2-loop level; left panel: comparison of the rates (as taken from Ref. ²⁰) obtained from a $\pi\rho$ gas¹⁰ (dashed lines) and $\pi\rho a_1$ gas within either the MYM¹⁹ (dotted lines) or the HLS framework²⁰ (solid lines); all calculations are without hadronic formfactors; right panel: $\pi\rho a_1$ system within HLS²¹ with (dashed lines) and without (solid lines) inclusion of hadronic vertex formfactors.

$T=100-200$ MeV, the predicted emission rates are inevitably beset with significant uncertainties, and therefore a careful judgment of the latter becomes mandatory.

Investigations along these lines were initiated in Ref. ¹⁰, where the photon self-energy has been computed to 2-loop order for a mesonic system consisting of sharp (zero width) π -, η - and ρ -mesons (plus direct $\omega \rightarrow \pi^0\gamma$ decays). The important processes were identified as $\pi\pi \rightarrow \rho\gamma$ at low energy ($q_0 \lesssim 0.5$ GeV) and $\pi\pi \rightarrow \rho\gamma$ at energies above ~ 0.8 GeV (both proceeding via one-pion-exchange and a contact graph), as well as ω decays around $q_0 \simeq 0.5$ GeV. It was also noted that effects of hadronic vertex formfactors could significantly affect the emission rates especially at high energies. In Ref. ¹⁸ it was pointed out that $\pi\rho \rightarrow \pi\gamma$ scattering via $a_1(1260)$ resonance formation (or, equivalently, $a_1 \rightarrow \pi\gamma$ decay) constitutes an important contribution. This was followed up by a systematic treatment¹⁹ of an interacting $\pi\rho a_1$ system to 2-loop order within the Massive Yang-Mills (MYM) framework of introducing axial-/vector mesons into a chiral Lagrangian, and, later, within the Hidden-Local Symmetry (HLS) approach²⁰. A compilation of rates from the $\pi\rho \rightarrow \pi\gamma$ channel is shown in the left panel of Fig. 2. The larger results of the MYM calculation as compared to the HLS one can be traced back to a significantly larger $a_1 \rightarrow \pi\gamma$ decay branching (which, in fact, overestimates the empirical value). Indeed, a recent MYM calculation²¹ with a smaller $\Gamma_{a_1 \rightarrow \pi\gamma}$ is consistent with the previous HLS one, cf. right panel of Fig. 2. One should remark, however, that a consistent and accurate vacuum phenomenology of the $\pi\rho a_1$ system (including radiative and hadronic a_1 decays, as well as the D/S ratio for the latter) has not been achieved yet. Also illustrated in the right panel of Fig. 2 is the impact of hadronic formfactors²¹. As anticipated, a substantial reduction of the rate is found, reaching a factor 3-4 in the

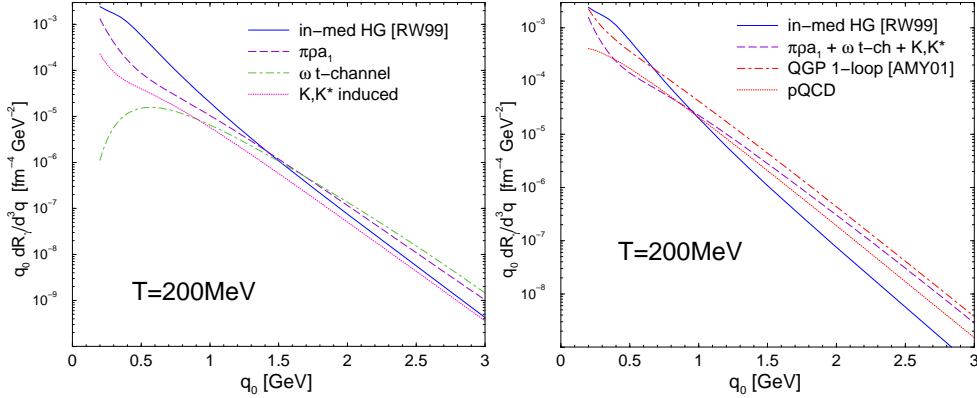
6 *Ralf Rapp*

Fig. 3. Left panel: thermal photon production channels in hot and dense hadronic matter²¹ under conditions resembling URHICs at SPS energy; right panel: total hadronic emission rates (sum of "in-med HG" [solid line] and perturbative mesonic channels [dashed line]) compared to QGP ones (either the Born rate, Eq. (3), or the complete leading order one, Eq. (4)).

2-3 GeV range, which should be included in quantitative analyses.

Photon production from strangeness bearing mesons and baryonic matter has been studied in Ref. ²¹. Within a HLS approach extended to flavor- $SU(3)$, K - and K^* -induced reactions contribute at the 40-50% level of the $\pi\rho a_1$ gas²¹, cf. left panel of Fig. 3 (see also Ref. ²²). Baryonic processes have been extracted from an in-medium ρ -meson spectral function²³ via Eq. (1), being quantitatively constrained by photoabsorption cross sections on nuclei²⁴. Under conditions resembling A - A collisions at the SPS, they constitute the dominant source of photons below $q_0 \simeq 1$ GeV. Similar conclusions were reached in the chiral reduction formula framework²⁵, whereas in Ref. ²⁶ baryonic contributions were found to be negligible for net-baryon free matter (note that the photon selfenergy depends on the *sum* of baryon and antibaryon densities which are not very different at SPS and RHIC energies). A surprisingly large photon yield has been identified in Ref. ²¹ as being due to ω t -channel exchange in $\pi\rho \rightarrow \pi\gamma$, rendering it the single most important process for energies beyond 2 GeV, after proper incorporation of hadronic formfactors (dash-dotted line in the left panel of Fig. 3). This result has been challenged in a recent comment²⁷, where, however, no hadronic formfactors were accounted for.

The impact of in-medium modified hadron properties has been studied in Refs. ^{29,30} in terms of reduced axial-/vector meson masses²⁸, leading to an increase of photon rates by up to a factor ~ 10 close to T_c . In Ref. ²⁰ it has been argued within the HLS approach that in-medium coupling constants should also decrease, which resulted in a small net change compared to the vacuum rates. Many-body effects on in-medium vector spectral functions are automatically incorporated when carrying the correlator to the photon point (solid lines in Fig. 3).

Finally, we compare in the right panel of Fig. 3 QGP with HG emission: in

the expected phase transition region, the top-down extrapolated partonic rates (especially for the complete LO case) are very close to the bottom-up extrapolated hadronic ones, quite reminiscent to earlier results for thermal dilepton rates³.

3. Current Status of Heavy-Ion Phenomenology

To evaluate the role of thermal photon radiation in high-energy heavy-ion collisions, an assessment of competing sources in the experimental spectra is required. Since final-state hadron decays (most notably $\pi^0, \eta \rightarrow \gamma\gamma$) are routinely removed from the measured spectra, the remaining nonthermal sources are essentially due to primary N - N collisions and subsequent early evolution phases during which the matter has not yet thermalized. We will briefly discuss these sources in the following Section before turning to the discussion of currently available data.

3.1. Non-Thermal Sources

Photons produced in hard (primary) N - N collisions (so-called "prompt" photons) are calculable from perturbative QCD at sufficiently large transverse momentum (where they are also expected to be most relevant, due to their power-law type spectra). Invoking the QCD factorization theorem, the photon-producing processes are in principle the same as in the QGP (recall left panel of Fig. 1), but now convoluted over the parton distribution functions (PDF's) of the incoming hadrons. An additional component is due to Bremsstrahlung processes in the fragmentation of a hard scattered parton, where the corresponding fragmentation function is not under good control yet^{32,7}. Nevertheless, a satisfactory description of prompt photon data in p - p collisions is possible, without having to introduce an intrinsic k_t broadening in the nucleon PDF's. In p - A collisions, additional nuclear effects occur, most notably the Cronin effect (also known as nuclear k_t -broadening) and shadowing of the PDF's. Whereas the former is most relevant (and experimentally well established) at fixed target energies ($\sqrt{s_{NN}} \leq 50$ GeV), the latter is likely to become increasingly important at high energies and forward rapidities, *i.e.*, low at x (as assessed, *e.g.*, in recent calculations employing gluon saturation ideas^{34,35}). Indeed, at SPS energies ($\sqrt{s} \leq 20$ GeV) the Cronin effect for prompt photons has been estimated to be rather significant^{36,37}, whereas for central rapidities at RHIC neither nuclear broadening nor shadowing appear to be particularly prominent.

The second nonthermal source in the early phases of URHICs is generically called the "pre-equilibrium" contribution which is theoretically rather difficult to evaluate. In both hadronic and partonic frameworks one key quantity is the formation time, either for building up hadronic wave functions, or for the thermalization of the QGP. The uncertainty of pre-thermal yields also pertains to their dependence on (transverse) momentum, as one does not expect (hadronic or partonic) modes to thermalize beyond a certain regime in p_t (as borne out of hadronic spectra at RHIC (see, *e.g.*, Ref. ³¹), especially their azimuthal asymmetries). One way

to study the pre-equilibrium phase is by using parton cascade (or transport) simulations in connection with pQCD cross section (and quark fragmentation) for photon production^{38,39}. The main problem in this framework is that many-body effects, *e.g.*, quantum interference (LPM suppression) or color screening (required for infrared regularization), are not easily implemented in a controlled way. This can, in principle, be improved within a quantum-field theoretical real-time formulation of an evolving partonic phase, as has been pursued in Ref. ⁴⁰. Here, one of the challenges is a realistic description of the bulk space-time dynamics of the expanding system, starting from the incoming nuclei.

Another conceivable nonthermal contribution can arise from hard partons propagating through the QGP⁴¹, via either jet-photon conversion (gluon Compton scattering or anti-/quark annihilation) or Bremsstrahlung off a quark. Generally speaking, all three pre-/off-equilibrium contributions mentioned above lead to quite appreciable photon yields, as compared to thermal estimates, at momenta relevant for QGP radiation (cf. the following section).

3.2. *Comparison to Data and Interpretations*

With photons being emitted throughout the evolution of a heavy-ion collision, a realistic description of the latter is an important ingredient for determining the thermal yield, especially if one studies sensitivities to the early (QGP) phases. One possibility are transport calculations evaluating photon producing reactions on a process by process basis. The implementation of thermal production rates as discussed in Sect. 2 is, however, most appropriately done in the context of hydrodynamic simulations, which are formulated in the same variables as the rates (temperature and chemical potentials for conserved charges). The main inputs for relativistic hydrodynamics are (i) the total initial energy and its spatial profile (according to, *e.g.*, participant or primary-collision densities in the transverse plane), (ii) the initial 3-volume usually specified by the thermalization time τ_0 as $V_0 = \tau_0 \Delta y \pi R_t^2$ (R_t : transverse radius of the nuclear overlap for a given collision centrality), and, (iii) the equation of state governing the subsequent expansion, ideally taken from first principle lattice QCD (or in terms of suitable approximations thereof, *e.g.*, quasi-particle QGP plus resonance hadron gas, matched via a latent heat at the transition). With the total initial energy being largely constrained by the finally observed hadron multiplicities (or transverse energy), the key parameter in determining the QGP contribution is the thermalization time τ_0 , which directly converts into an initial temperature (note, however, that non-boost-invariant initial conditions in the longitudinal coordinate induce significant uncertainties in this relation, cf. Ref. ⁴²). The hydrodynamic equations are solved on a space-time grid, and the thermal photon yield is straightforwardly obtained by multiplying the emission rate with the space-time (eigen-) volume of each unit cell at given local temperature and density.

An early measurement of photons in URHICs was performed by the WA80 collaboration in $S(200\text{A GeV})$ - Au collisions at the SPS, resulting in upper limits on the

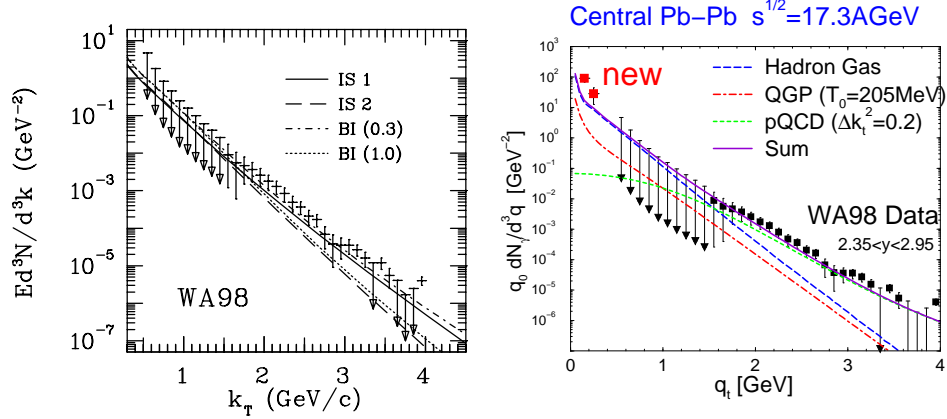


Fig. 4. Direct photon spectra as measured by WA98^{46,47} in central $Pb(158 \text{ AGeV})+Pb$ collisions at the SPS. Left panel: hydrodynamic calculations of thermal photon spectra⁴² (including both QGP and HG emission) assuming various initial conditions (dotted and dash-dotted line: boost invariant for $\tau_0=1$ and 0.3 fm/c , respectively; long-dashed and solid line: non-boost invariant longitudinal flow distributions with average initial temperatures of $\bar{T}_0 \simeq 215$ and 255 MeV , respectively); right panel: expanding thermal fireball calculations with average initial temperature $\bar{T}_0 \simeq 205 \text{ MeV}$, supplemented with an initial pQCD yield that includes nuclear k_t -broadening²¹.

direct photon yield⁴³. The theoretical consensus was that in these reactions initial temperatures in excess of 250 MeV could be excluded^{44,45}. The successor experiment WA98 succeeded in obtaining a nonzero signal resulting in the direct-photon q_t -spectra⁴⁶ as shown in Fig. 4. In the left panel, the data are compared to hydrodynamic calculations⁴² which include both QGP and hadronic phase with a transition at $T_c=165 \text{ MeV}$, employing complete leading order emission rates in the QGP¹⁴ and a HG rate based on $\pi\pi \rightarrow \rho\gamma$ and $\pi\rho \rightarrow \pi\gamma$ according to Refs. 10,18 (including π and s -channel a_1 exchanges). The comparison of different initial states (non-/boost invariant, with formation times of 0.3 and 1.0 fm/c) indicates that a satisfactory description of the WA98 in terms of thermal radiation (without contributions from primary N - N collisions) requires rather large initial temperatures $T_0^{max} \simeq 330 \text{ MeV}$ (translating into $\bar{T}_0 \simeq 260 \text{ MeV}$ when averaged over the transverse plane), rendering the QGP radiation the dominant source (similar results have been obtained in Ref. 48). These conclusions are not significantly altered if the primordial pQCD yield is added in terms of N - N collision-scaled spectra from p - p collisions. The situation changes if the latter contribution is augmented by accounting for the Cronin effect, cf. right panel of Fig. 4. With a rather moderate nuclear k_t -broadening, the initial pQCD yield increases by about a factor of 2-3 in the $q_t=2-4 \text{ GeV}$ range, and thus turns out to saturate the experimental spectra for $q_t > 2.5 \text{ GeV}$. Consequently, the role of the thermal yield, which has been modeled in a more simplistic thermal fireball evolution, is diminished. With the same underlying QGP emission rates as in the hydrodynamic calculation (but a more complete description of the

hadronic rates²¹) the data are compatible with significantly smaller (average) initial temperatures of $\bar{T}_0 \simeq 205$ MeV (corresponding to $\tau_0 \simeq 1$ fm/c), rendering the QGP contribution subdominant in the relevant range $q_t \leq 2.5$ GeV. In fact, this can also be expected to hold for the hydrodynamic calculations.

A rather dramatic addition to the WA98 data has recently been provided at low transverse momenta ($q_t = 100\text{--}300$ MeV, labeled "new" in the right panel of Fig. 4), extracted via $\gamma\text{--}\gamma$ HBT interferometry techniques⁴⁷ (which automatically eliminate late hadron decays, most notably $\pi^0, \eta \rightarrow \gamma\gamma$). The default thermal calculations underestimate these data by a rather substantial margin. Some improvement arises when including soft $\pi\pi \rightarrow \pi\pi\gamma$ Bremsstrahlung, via S -wave $\pi\pi$ interactions⁴⁹ (which are suppressed at higher q_t). Additional hadronic processes with large yields are not easily conceivable. Increasing the fireball lifetime by, *e.g.*, 30%, implying lower thermal freezeout temperatures $T_{fo} \simeq 90$ MeV (to be compared to standard values of ~ 110 MeV), increases the thermal contribution at low q_t by about the same fraction. This raises the exciting possibility that one is observing substantial in-medium modifications, *e.g.*, a reduced " σ "-mass in the S -wave $\pi\pi$ interaction. A possibly related phenomenon may have been observed in π^- - and γ -induced 2π production experiments off ground state nuclei^{50,51,52,53}. The measured invariant-mass distributions in the scalar-isoscalar channel exhibit appreciable shifts of strength towards the 2-pion threshold when going from hydrogen to heavy nuclear targets (no such effect is observed in the pure isotensor $\pi^+\pi^+$ final-state where the (strong) $\pi\pi$ interaction is repulsive), despite expected pion absorption (which biases pion emission towards the nuclear surface, *i.e.*, rather small densities). A similar softening in the $\pi^-\pi^+$ interaction in the heavy-ion environment, where additional thermal occupation factors appear, could induce a substantial soft-photon enhancement⁴⁹. Another possibility are medium modifications of the $\Delta(1232)$ resonance⁵⁴, which has a large radiative branching ratio.

Direct photon spectra as predicted for central $Au\text{--}Au$ collisions at RHIC energy are compiled in the left panel of Fig. 5⁵⁵. Thermal radiation from two different approaches, *i.e.*, hydrodynamic^{7,56} (solid line, for formation time $\tau_0 = 0.18$ fm/c) and expanding fireball²¹ (long-dashed line, for formation time $\tau_0 = 0.33$ fm/c), is in approximate agreement with each other (the 2 curves also include primordial pQCD contributions). In both calculations QGP radiation dominates for transverse momenta above $q_t \simeq 1$ GeV. Whereas in the fireball expansion the QGP has been assumed to be in chemical equilibrium, the hydrodynamic evolution incorporates an undersaturation of gluons and especially quarks (which is motivated by the predominance of low- x gluons in the wave function of the incoming nucleons, and represented by initial fugacities $\lambda_{q,\bar{q},g} < 1$, evolved in time) in both equation of state and QGP emission rates^{7,56}. Compared to the chemical equilibrium case, parton undersaturation implies reduced emission rates, but also larger initial temperatures if the initial entropy, which determines the number of produced particles, is fixed. It turns out that, to a large extent, these two effects compensate each other⁷.

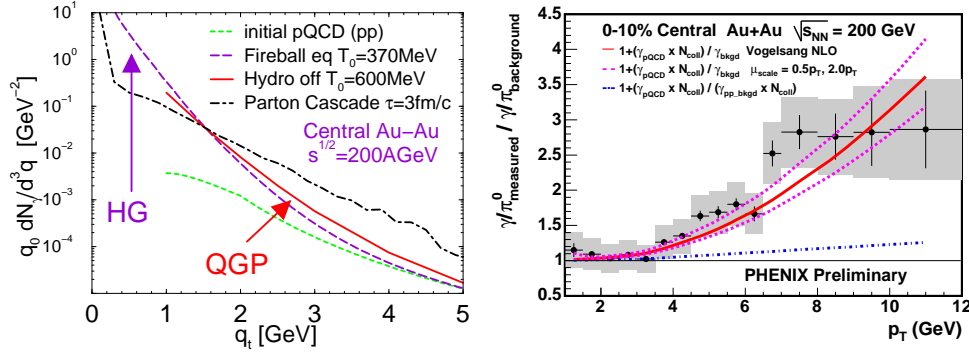


Fig. 5. Left panel: compilation⁵⁵ of direct photon yields for central $Au-Au$ collisions at RHIC: hydrodynamic^{56,7} (solid line) and fireball²¹ (long-dashed line) calculations of thermal radiation including the yield from primordial pQCD photons⁵⁷ (shown also separately by the short-dashed line), as well as results from the first 3 fm/c of a parton cascade simulation³⁹ (dash-dotted line); right panel: direct photon data⁵⁸ from central $Au-Au$ at RHIC compared to next-to-leading order pQCD predictions⁵⁹ for primordial $N-N$ collisions (scaled by the number of hard collisions).

The primordial pQCD contribution in Fig. 5 (left panel) is taken from a parametrization⁵⁷ of $p-p$ data over a large range of center-of-mass energies, scaled by the number of $N-N$ collisions in central $Au-Au$, and without Cronin effect (expected to be rather small at RHIC). Comparison with the thermal contribution indicates that the latter can compete up to $q_t \simeq 5$ GeV. The dash-dotted line in Fig. 5 (left panel) represents an estimate of photon production from parton rescattering and fragmentation within the first 3 fm/c of a parton cascade model³⁹. The resulting photon yield exceeds both thermal and primordial pQCD yields by up to an order of magnitude for transverse momenta of around 4-5 GeV. In this regime, the contribution from jet- γ conversions⁴¹ (not shown in Fig. 5) turns out to be comparable in magnitude to the thermal+pQCD radiation.

In the right panel of Fig. 5 preliminary data from PHENIX⁵⁸ are displayed as a (double) ratio of measured photons over those expected from meson decays. Above $q_t \simeq 4$ GeV, this ratio significantly exceeds one, being attributed to direct photons, which are in good agreement with predictions for primordial pQCD photons⁵⁹. Currently there is not enough sensitivity to QGP radiation, but the large yields obtained in the parton cascade are disfavored.

The prospects of identifying thermal photon radiation in future heavy-ion collisions at the LHC ($Pb-Pb$ at $\sqrt{s}=5500$ AGeV) have been thoroughly assessed in a recent CERN Yellow Report⁷. These studies suggest that the window in which thermal photons exceed the pQCD production could extent up to almost $q_t=10$ GeV, with larger maximal enhancement factors than at RHIC.

4. High-Density Quark Matter

Besides high-energy heavy-ion collisions (and the early universe), the other systems in nature in which strongly interacting matter under extreme conditions is likely to exist are compact stars. Contrary to the high-temperature medium formed in URHICs, compact stars are characterized by high baryon densities at *low* temperatures. Nevertheless, much like for URHICs, electroweak emission spectra play an important role in inferring properties of the matter within the star. The main focus is traditionally on neutrinos⁶⁰, due to their substantially longer mean free path as compared to photons. Renewed interest in the electroweak emission spectra was generated when it was realized that color-superconducting quark matter (CSC) may exist with values for the quark-pairing as large as $\Delta \sim 100$ MeV^{61,62}, rendering them possibly relevant for phenomenological applications. Subsequently, both neutrino^{63,64,65,66} and photon^{67,68} emissivities have been assessed for CSC. Clearly, if CSC is limited to exist in the core of compact stars, pertinent photon signals cannot be observed. The latter can therefore only be relevant for (hypothetical) "strange quark matter" stars, in which quark matter extends all the way to the star's surface. Even in this case, not much is known as to how the surface structure impacts photon emission.

This notwithstanding, thermal photon rates from the so-called color-flavor-locked (CFL) phase⁶⁹ of CSC were calculated in Refs. ^{67,68}. In CFL matter, u , d and s quarks of approximately equal Fermi momenta form Cooper pairs in a way that breaks the original $SU(3)_C \times SU(3)_L \times SU(3)_R$ symmetry to a global $SU(3)$ one, implying (among other things) the emergence of 8 Goldstone bosons. The small explicit breaking due to the finite current quark masses induces corresponding pion masses $m_\pi \approx 10$ MeV (even smaller (larger) for (anti-) kaons). For temperatures (well) below this scale, Goldstone boson excitations are exponentially suppressed and photon emissivities are controlled by electromagnetic processes involving e^\pm and γ 's, provided an electrosphere forms at the star surface^{70,71} (this is, in fact, not required for a pure CFL star, which is electrically neutral without the presence of electrons). Here, we focus on situations where the strong-interaction degrees of freedom are active, *i.e.*, temperatures of order tens of MeV as characteristic for the early evolution phases following a supernova explosion.

The photon selfenergy in CSC has been computed in Ref. ⁷² at zero temperature and for asymptotic densities employing weak coupling techniques. The corresponding $q\bar{q}$ one-loop selfenergy in the CFL phase has been extended to finite temperatures and applied to photon emission rates using Eq. (1) in Ref. ⁶⁷. For temperatures $T \sim 70$ MeV and comparable baryon densities, the rates are quite similar to extrapolations of hadronic many-body calculations²³ (cf. Sect. 2.2).

In Ref. ⁶⁸, the notion of Goldstone bosons in the CFL phase has been exploited to formulate a HLS framework in the strong coupling regime. In addition, an in-medium pion dispersion relation⁷³, $\omega^2 = m_\pi^2 + v_\pi^2 p^2$ with $v_\pi^2 = 1/3$, was accounted for, leading to novel annihilation (and decay) processes of type $\pi^+ \pi^- \leftrightarrow \gamma$ (see also

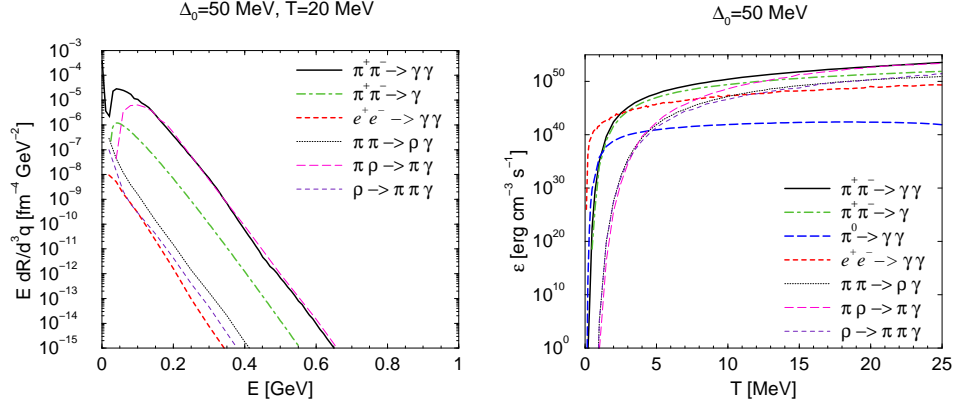


Fig. 6. Photon emission rates from CFL quark matter within a HLS approach (left panel), and corresponding (integrated) emissivities vs. temperature⁶⁸. The finite- T gap value has been assumed to follow the BCS relation $\Delta(T) = \Delta_0 \sqrt{1 - (T/T_c)^2}$ with $T_c = 0.57\Delta_0$.

Ref. ⁶⁶). With a ρ -meson mass of $\sim 2\Delta$ ⁷⁴, and assuming VDM, the gauge coupling was found to be $\tilde{g} = g_{\rho\pi\pi} \simeq 2$, significantly smaller than its vacuum value of ~ 6 . The rates and their integrated emissivities in Fig. 6 indicate that processes induced by Goldstone bosons dominate over e^+e^- annihilation at temperatures as low as 5 MeV; even strong-interaction processes involving ρ mesons may become irrelevant for temperatures $T \simeq 20$ MeV, and thus for newborn compact stars. In particular, the results for photon mean-free-path and emissivity imply that the photon flux from a (hypothetical) hot CFL star saturates the black-body limit.

5. Conclusions

In recent years significant progress has been made in our attempts to address the question: what is the electromagnetic blackbody spectrum of strong-interaction matter at given temperature and density? In the QGP phase, the role of soft t -channel exchanges has been understood better, leading to a photon emission rate that constitutes the full result to leading order in α_s . In the hadronic phase, existing calculations could be refined and supplemented by additional processes towards a more complete description. Clearly, in the vicinity of the expected (pseudo-) phase transition neither current partonic nor hadronic calculations are quantitatively reliable, but the fact that they agree within, say, a factor of two over a large range of energies (over which the rate itself changes by several orders of magnitude), increases the confidence in both calculations, and may eventually teach us something about the phase transition itself. Fully nonperturbative results from (unquenched) QCD lattice calculations are eagerly awaited. Moreover, phenomenological applications to (ultra-) relativistic heavy-ion collisions compare favorably to existing data (except the new low-momentum data from WA98), further corroborating the (approximate)

validity of theoretical estimates. At the SPS, most approaches agree that temperatures in excess of the critical one are required in the early phases of head-on $Pb-Pb$ collisions. This adds significantly to similar evidence gained from dilepton spectra. At RHIC, the QGP signal is expected to become substantially stronger, but so do prompt photon yields from initial hard collisions. Up to now, electromagnetic signals from URHIC's have never failed to generate excitement.

Acknowledgments

It is a pleasure to thank C. Gale, P. Jaikumar, R. Ouyed, S. Turbide, C. Vogt and I. Zahed for enjoyable and stimulating collaboration on the presented topics. Interesting discussions with T. Awes and K. Haglin are also acknowledged.

1. E.L. Feinberg, *Nuovo Cim.* **A34**, 391 (1976).
2. E.V. Shuryak, *Sov. J. Nucl. Phys.* **28**, 408 (1978).
3. R. Rapp and J. Wambach, *Adv. Nucl. Phys.* **25**, 1 (2000).
4. J. Alam, S. Sarkar, P. Roy, T. Hatsuda, B. Sinha, *Ann. Phys.* **286**, 159 (2001).
5. T. Peitzmann and M. Thoma, *Phys. Rep.* **364**, 175 (2002).
6. C. Gale and K. Haglin, in R.C. Hwa *et al.* (ed.), *Quark Gluon Plasma*, 364 (2004), and arXiv:hep-ph/0306098.
7. F. Arleo *et al.*, writeup of *Photon Physics* working group for CERN Yellow Report on *Hard Probes in Heavy Ion Collisions at the LHC*, arXiv:hep-ph/0311131 v3.
8. K. Kajantie and H.I. Miettinen, *Z. Phys.* **C9**, 341 (1981).
9. K. Kajantie and P.V. Ruuskanen, *Phys. Lett.* **B121**, 352 (1983).
10. J. Kapusta, P. Lichard and D. Seibert, *Phys. Rev.* **D44**, 2774 (1991); erratum *ibid.* **D47**, 4171 (1993).
11. R. Baier, H. Nakagawa, A. Niegawa, K. Redlich, *Z. Phys.* **C53**, 433 (1992).
12. P. Aurenche, F. Gelis, R. Kobes and H. Zaraket, *Phys. Rev.* **D58**, 085003 (1998).
13. F.D. Steffen and M.H. Thoma, *Phys. Lett.* **B510**, 98 (2001).
14. P. Arnold, G.D. Moore and L.G. Yaffe, *JHEP* 0112, 009 (2001).
15. C.T. Traxler, H. Vija and M.H. Thoma, *Phys. Lett.* **B346**, 329 (1995).
16. F. Karsch and E. Laermann, in R.C. Hwa *et al.* (ed.), *Quark gluon plasma*, 1 (2004), and arXiv:hep-lat/0305025.
17. E. Braaten, R.D. Pisarski and T.-C. Yuan, *Phys. Rev. Lett.* **64**, 2242 (1990).
18. L. Xiong, E.V. Shuryak and G.E. Brown, *Phys. Rev.* **D46** (1992) 3798.
19. C. Song, *Phys. Rev.* **C47**, 2861 (1993).
20. M.-A. Halasz, J.V. Steele, G.Q. Li and G.E. Brown, *Phys. Rev.* **C58**, 365 (1998).
21. S. Turbide, R. Rapp and C. Gale, *Phys. Rev.* **C69**, 014903 (2004).
22. K.L. Haglin, arXiv:hep-ph/0308084.
23. R. Rapp and J. Wambach, *Eur. Phys. J.* **A6** (1999) 415.
24. R. Rapp, M. Urban, M. Buballa and J. Wambach, *Phys. Lett.* **B417** (1998) 1.
25. J.V. Steele and I. Zahed, *Phys. Rev.* **D60** (1999) 037502.
26. J. Alam, P. Roy and S. Sarkar, *Phys. Rev.* **C68** (2003) 031901.
27. J. Alam, P. Roy and S. Sarkar, arXiv:hep-ph/0310168.
28. G.E. Brown and M. Rho, *Phys. Rep.* **269** (1996) 333.
29. C. Song and G. Fai, *Phys. Rev.* **C58** (1998) 1689.
30. J. Alam, P. Roy, S. Sarkar and B. Sinha, *Phys. Rev.* **C67** (2003) 054901.
31. Proceedings of the 17. International Conference on Ultrarelativistic Nucleus-Nucleus

- Collisions, *Quark Matter 2004* (Oakland, CA, Jan. 11-17, 2004), to be published in J. Phys. **G**.
32. L. Bourhis, M. Fontannaz and J.P. Guillet, Eur. Phys. J. **C2** (1998) 529.
 33. P. Aurenche, M. Fontannaz, J.P. Guillet, B. Kniehl, E. Pilon and M. Werlen, Eur. Phys. J. **C9** (1999) 107.
 34. F. Gelis and J. Jalilian-Marian, Phys. Rev. **D66** (2002) 014021.
 35. R. Baier, A.H. Mueller and D. Schiff, arXiv:hep-ph/0403201.
 36. G. Papp, P. Levai and G. Fai, Phys. Rev. **C61** (1999) 021902.
 37. A. Dumitru, L. Frankfurt, L. Gerland, H. Stöcker and M. Strikman, Phys. Rev. **C64** (2002) 054909.
 38. D.K. Srivastava and K. Geiger, Phys. Rev. **C58** (1998) 1734.
 39. S.A. Bass, B. Müller and D.K. Srivastava, Phys. Rev. Lett. **90** (2003) 082301.
 40. D. Boyanovsky and H.J. de Vega, Phys. Rev. **D68** (2003) 065018.
 41. R.J. Fries, D.K. Srivastava and B. Müller, Phys. Rev. Lett. **90** (2003) 132301.
 42. P. Huovinen, P.V. Ruuskanen and S.S. Räsänen, Phys. Lett. **B535** (2002) 109.
 43. WA80 Collaboration (R. Albrecht *et al.*), Phys. Rev. Lett. **76** (1996) 3506.
 44. A. Dumitru *et al.*, Phys. Rev. **C51** (1995) 2166.
 45. D.K. Srivastava and B.C. Sinha, Eur. Phys. J. **C12** (2000) 109, erratum-ibid. **C20** (2001) 397.
 46. WA98 Collaboration (M.M. Aggarwal *et al.*), Phys. Rev. Lett. **85** (2000) 3595.
 47. WA98 Collaboration (M.M. Aggarwal *et al.*), arXiv:nucl-ex/0310022.
 48. D.K. Srivastava and B. Sinha, Phys. Rev. **C64** (2001) 034902.
 49. S. Turbide, C. Gale and R. Rapp, work in progress.
 50. CHAOS Collaboration (F. Bonutti *et al.*), Phys. Rev. Lett. **77** (1996) 603.
 51. Crystal Ball Collaboration (A. Starostin *et al.*), Phys. Rev. Lett. **86** (2000) 5539.
 52. TAPS Collaboration, (J.G. Messchendorp *et al.*), Phys. Rev. Lett. **89** (2002) 222302.
 53. See, *e.g.*, T. Kunihiro, arXiv:nucl-th/0403002, and references therein.
 54. H. van Hees and R. Rapp, in preparation.
 55. R. Rapp, arXiv:nucl-th/0403048.
 56. F. Gelis, H. Niemi, P.V. Ruuskanen and S.S. Räsänen, arXiv:nucl-th/0403040.
 57. D.K. Srivastava, Eur. Phys. J. **C22** (2001) 129.
 58. PHENIX Collaboration (J. Frantz *et al.*), arXiv:nucl-ex/0404006.
 59. S. Catani, M.L. Mangano, P. Nason, C. Oleari and W. Voglesang, JHEP 9903, 025 (1999).
 60. M. Prakash, J.M. Lattimer, R.F. Sawyer and R.R. Volkas, Annu. Rev. Nucl. Part. Sci. **51** (2001) 295.
 61. R. Rapp, T. Schäfer, E.V. Shuryak and M. Velkovsky, Phys. Rev. Lett. **81** (1998) 51.
 62. M. Alford, K. Rajagopal and F. Wilczek, Phys. Lett. **B422** (1998) 247.
 63. D. Blaschke, T. Klahn and D.N. Voskresensky, Astrophys. J. **533** (2000) 2048.
 64. D. Page, M. Prakash, J.M. Lattimer and A. Steiner, Phys. Rev. Lett. **85** (2000) 2048.
 65. P. Jaikumar, M. Prakash and T. Schäfer, Phys. Rev. **D66** (2002) 063003.
 66. S. Reddy, M. Sadzikowski and M. Tachibana, Nucl. Phys. **A714** (2003) 337.
 67. P. Jaikumar, R. Rapp and I. Zahed, Phys. Rev. **C65** (2002) 055205.
 68. C. Vogt, R. Rapp and R. Ouyed, Nucl. Phys. **A735** (2004) 543.
 69. M. Alford, K. Rajagopal and F. Wilczek, Nucl. Phys. **B537** (1999) 443.
 70. D. Page and V.V. Usov, Phys. Rev. Lett. **89** (2002) 131101.
 71. P. Jaikumar, C. Gale, D. Page, M. Prakash, arXiv:astro-ph/0403427
 72. D.F. Litim and C. Manuel, Phys. Rev. **D64** (2001) 094013.
 73. D.T. Son and M.A. Stephanov, Phys. Rev. **D61** (2000) 074012; erratum-ibid. **62** (2000) 059902.

16 *Ralf Rapp*

74. M. Rho, E.V. Shuryak, A. Wirzba and I. Zahed, Nucl. Phys. **A676** (2000) 273.